

## RESEARCH LETTER

10.1002/2015GL064322

## Key Points:

- Quantify how Antarctic bed elevation uncertainty affects ice sheet simulations
- Simulate retreat of the Antarctic ice sheet for a warm Pliocene climate
- Identify key areas for future improvements to bed elevation data

## Supporting Information:

- Text S1 and Figures S1–S3

## Correspondence to:

E. Gasson,  
egw.gasson@gmail.com

## Citation:

Gasson, E., R. DeConto, and D. Pollard (2015), Antarctic bedrock topography uncertainty and ice sheet stability, *Geophys. Res. Lett.*, 42, 5372–5377, doi:10.1002/2015GL064322.

Received 1 MAY 2015

Accepted 24 JUN 2015

Accepted article online 27 JUN 2015

## Antarctic bedrock topography uncertainty and ice sheet stability

E. Gasson<sup>1</sup>, R. DeConto<sup>1</sup>, and D. Pollard<sup>2</sup>
<sup>1</sup>Climate System Research Center, University of Massachusetts Amherst, Amherst, Massachusetts, USA, <sup>2</sup>Earth and Environmental Systems Institute, Pennsylvania State University, University Park, State College, Pennsylvania, USA

**Abstract** Antarctic bedrock elevation estimates have uncertainties exceeding 1 km in certain regions. Bedrock elevation, particularly where the bedrock is below sea level and bordering the ocean, can have a large impact on ice sheet stability. We investigate how present-day bedrock elevation uncertainty affects ice sheet model simulations for a generic past warm period based on the mid-Pliocene, although these uncertainties are also relevant to present-day and future ice sheet stability. We perform an ensemble of simulations with random topographic noise added with various length scales and with amplitudes tuned to the uncertainty of the Bedmap2 data set. Total Antarctic ice sheet retreat in these simulations varies between 12.6 and 17.9 m equivalent sea level rise after 3 kyrs of warm climate forcing. This study highlights the sensitivity of ice sheet models to existing uncertainties in bedrock elevation and the ongoing need for new data acquisition.

## 1. Introduction

Bedrock elevation is an important boundary condition for ice sheet models. The recently released Bedmap2 data set has bedrock elevation uncertainties exceeding 1 km in certain regions [Fretwell *et al.*, 2013]. Obtaining high-resolution bedrock elevation data typically requires costly airborne geophysical surveys, often in remote regions of the Antarctic. Prioritizing where to focus these efforts is of importance [Pritchard, 2014]. A recent survey of experts from various communities with an interest in polar science identified regions where improved bedrock elevation data are needed [Pritchard, 2014]. However, there have been limited attempts to quantify the impact of bedrock elevation uncertainty on ice sheet models [Sun *et al.*, 2014], which could provide a more objective way of identifying regions where surveying resources should be prioritized.

The magnitudes of bedrock elevation uncertainty for the Bedmap2 data set (shown in Figure 1) are typically less than ~325 m; however, in regions where direct ice thickness measurements are unavailable, bedrock elevation uncertainty can greatly exceed this [Fretwell *et al.*, 2013]. The largest bedrock elevation uncertainty is in East Antarctica, including two broad regions of high uncertainty: the region between Recovery and Support Force glaciers, and Princess Elizabeth Land. A large proportion of the East Antarctic ice sheet (EAIS) is grounded below sea level, loss of which has the potential to raise sea level by 19.2 m [Fretwell *et al.*, 2013]. Ice flux at the grounding line is strongly dependent on ice thickness there [Schoof, 2007], meaning that runaway retreat can occur for marine-based regions where the bedrock elevation deepens upstream [Weertman, 1974; Mercer, 1978; Schoof, 2007] (the “marine ice sheet instability”). Simulation of the marine ice sheet instability requires accurate bedrock elevation data, often at very high resolution [Gladstone *et al.*, 2012; Pattyn *et al.*, 2013; Sun *et al.*, 2014].

Another ice sheet instability mechanism recently suggested by Bassis and Walker [2011] and explored in an ice sheet modeling study by Pollard *et al.* [2015], may also be strongly sensitive to uncertainties in bedrock elevation. In warm climate simulations (the mid-Pliocene warm period, ~3 Ma, was chosen in the study of Pollard *et al.* [2015], also see background in the supporting information) ice shelves can be removed by hydrofracturing as rainwater and surface meltwater drains into crevasses [Nick *et al.*, 2010; Pollard *et al.*, 2015]. The removal of ice shelves can exceed the rate at which ice is replenished with flow from surrounding ice streams and can result in tidewater glaciers terminating as sheer ice cliffs. At some height these ice cliffs will become structurally unstable resulting in ice cliff failure [Bassis and Walker, 2011; Pollard *et al.*, 2015]. The model of Pollard *et al.* [2015] assumes that ice is exactly at floatation at the grounding line; therefore, the cliff height is directly related to water depth and hence bedrock elevation. The ice cliff failure mechanism is parameterized using a

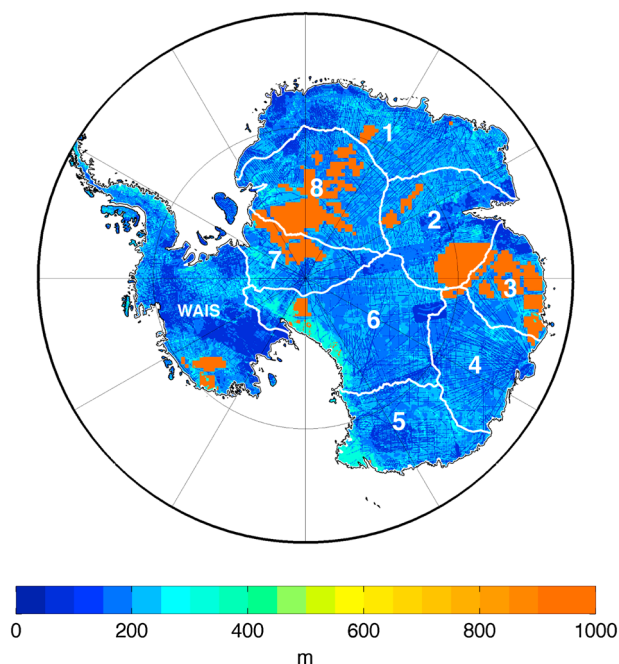


**Figure 1.** Bed elevation uncertainty for the Bedmap2 data set [Fretwell *et al.*, 2013]. The areas of high uncertainty ( $\sim 1000$  m) have no direct ice thickness measurement. Also marked on the map for the East Antarctic are large-scale drainage divides used in Figure 4, based partially on ICESat drainage system boundaries. The Aurora and Wilkes subglacial regions are within catchments 4 and 5, respectively.

wastage rate as a function of ice cliff height [Pollard *et al.*, 2015], as such the retreat rate is sensitive to bedrock elevation uncertainty.

Here we investigate how bedrock elevation uncertainties in the Bedmap2 data set [Fretwell *et al.*, 2013] affect ice sheet stability in an ice sheet model accounting for marine ice sheet instability, enhanced ice shelf hydrofracture, and ice cliff failure [Pollard *et al.*, 2015]. We investigate how this uncertainty affects simulations of mid-Pliocene warm period ice sheet dynamics, as this is a period with atmospheric  $\text{CO}_2$  concentrations similar to the present (400 ppm) [Seki *et al.*, 2010] with evidence for large-scale retreat of both the West and East Antarctic ice sheets [Naish *et al.*, 2009; Cook *et al.*, 2013; Raymo *et al.*, 2011]. Although we explore ice sheet sensitivity to bedrock elevation uncertainty for a mid-Pliocene climate forcing, these uncertainties are also relevant to simulations of future ice sheet dynamics for a projected warmer climate [Collins *et al.*, 2013].

## 2. Methods

To investigate how bedrock elevation uncertainty may affect ice sheet model simulations, we create multiple bedrock topographies which include random topographic noise. Random 2-D noise is created which is then filtered using a Gaussian low-pass filter, preserving various spatial frequencies and creating random topography at various length scales (from tens to hundreds of kilometers; similar to Sun *et al.* [2014]). We tune the amplitude of the topographic noise such that the majority of the noise ( $\pm 2$  standard deviations) falls within the bounds of each Bedmap2 uncertainty level, for the entire domain. The topographic noise is then added to the best estimate topography (i.e., Bedmap2), and ice thicknesses are adjusted to preserve surface ice elevations. From this, we create 40 topographies filtered at four different frequencies (Figure 2). The scale and magnitude of the random topographic noise produced is similar to the differences between the Bedmap1 and Bedmap2 data sets (see Figure S1), suggesting that producing random topographic noise in this manner is a reasonable approach to estimating the ice sheet sensitivity to bedrock elevation uncertainty.

The ice sheet model is documented in Pollard *et al.* [2015] and includes detailed discussion of the new hydrofracture and ice cliff failure mechanisms. An earlier version of the ice sheet model, without these new mechanisms, is also used and is documented in Pollard and DeConto [2012a]. We refer to the two versions of the ice sheet model as PDA15 and PD12.

Pollard and DeConto [2012b] tuned the basal sliding parameters within the ice sheet model to minimize present-day ice surface elevation errors using an inverse method. This inversion is sensitive to bedrock elevation uncertainties of the magnitude present in the Bedmap2 data set [Pollard and DeConto, 2012b], and as such, we repeat this inversion for all 40 of the topographies. The inversion uses present-day observed climatology, and the ice sheet model is run for 200 kyrs to equilibrate. Following this inversion, mean absolute surface elevation errors are below 70 m for all runs. This inversion is performed with the PDA15 version of the model, although similar basal sliding parameters are generated with the PD12 version of the model. We also perform tests without this inversion to determine whether the model is sensitive to the difference in topography or the basal sliding parameters.

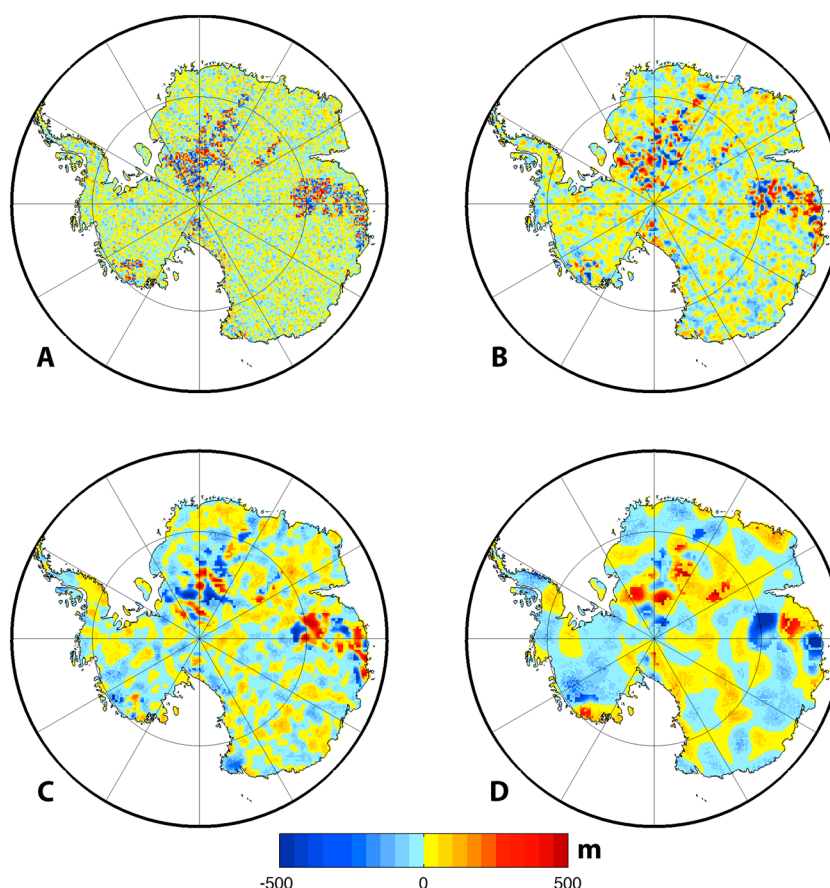


**Figure 2.** Examples of topographic noise. Random noise is filtered by Fourier methods with a Gaussian filter

$H(u, v) = \frac{1}{N^2} e^{-\frac{(u^2 + v^2)}{2\sigma^2}}$ , where  $N$  is the length of each side of the Bedmap2 domain (6667 km),  $u$  and  $v$  extend from  $-3333$  to  $3333$  km, and  $\sigma$  is (a) 10, (b) 25, (c) 50, and (d) 100. The random noise is then tuned for each uncertainty level such that  $\pm 2$  standard deviations of the amplitudes of the random noise are equal to the topography uncertainty, creating the topographic noise. Topographic noise is created at the resolution of the Bedmap2 data set (1 km) and then interpolated to the ice sheet model grid resolution (20 km), which may additionally smooth some features. The examples shown here are at 20 km grid resolution.

We first run the ice sheet model with a preindustrial control Regional Climate Model (RCM; RegCM3 [Pal et al., 2007]) forcing for 5 kyrs before switching to a generic warm mid-Pliocene climate. For these sensitivity studies we apply an instantaneous warm climate forcing. The RCM is modified for application to the polar regions, with boundary forcing from the GENESIS v3.0 Global Climate Model (GCM) [Thompson and Pollard, 1997; DeConto et al., 2012]. The generic warm mid-Pliocene climate forcing has an atmospheric  $\text{CO}_2$  concentration of 400 ppm and a very warm austral summer orbital configuration [DeConto et al., 2012; Pollard et al., 2015]. As detailed simulation of sub-ice shelf warming is currently not feasible on these timescales, a uniform ocean warming of  $2^\circ\text{C}$ , based on Pliocene reconstructions for the circum-Antarctic [Dowsett et al., 2009], is added to a present-day observed data set (NODC\_WOA98 data provided by the NOAA, Physical Sciences Division, Boulder, Colorado, USA), we acknowledge that this approach may not fully represent dynamical changes in ocean temperatures during the Pliocene. This subsurface ocean temperature data set is used to calculate sub-ice shelf melting parameterized using a quadratic function [Holland et al., 2008; Pollard and DeConto, 2012a], while sea surface temperatures are simulated by the GCM and RCM.

In previous ice sheet model simulations forced with this warm climate the West Antarctic Ice Sheet (WAIS) collapses (with and without the enhanced ice shelf hydrofracture and ice cliff failure mechanisms), therefore, the RCM boundary conditions assume that the WAIS is already collapsed. The GCM and RCM are used to calculate sea surface temperatures in the resulting West Antarctic seaways, accounting for feedbacks between the ice sheet and atmospheric temperatures. Subsurface temperatures are based on the nearest ocean cell to the ice sheet model grid point. A simple lithosphere flexure model accounts for changes in local sea level

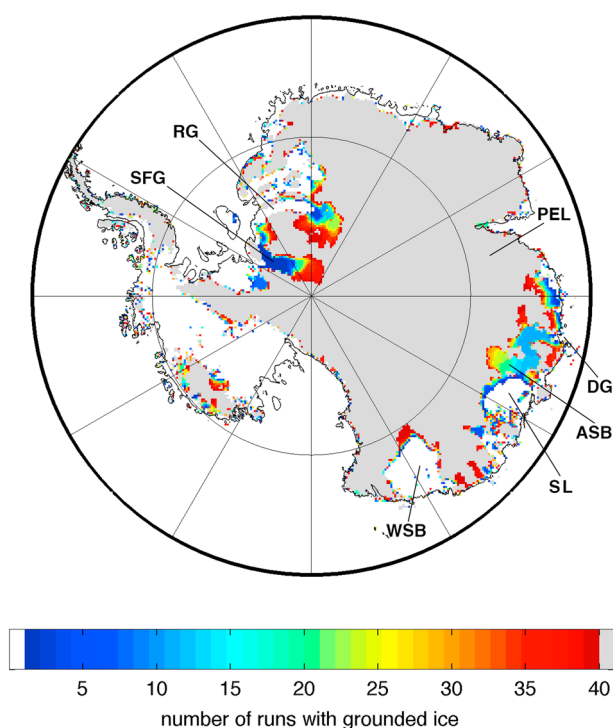


**Figure 3.** Number of simulations (out of 40) with grounded ice after 3 kyrs and forced with warm Pliocene climate, using PDA15 version of ice sheet model. Black outline is the present-day grounding line. Approximate location of areas referred to in the text: RG = Recovery Glacier; SFG = Support Force Glacier; PEL = Princess Elizabeth Land; DG = Denman Glacier; ASB = Aurora Subglacial Basin; SL = Sabrina Land; WSB = Wilkes Subglacial Basin.

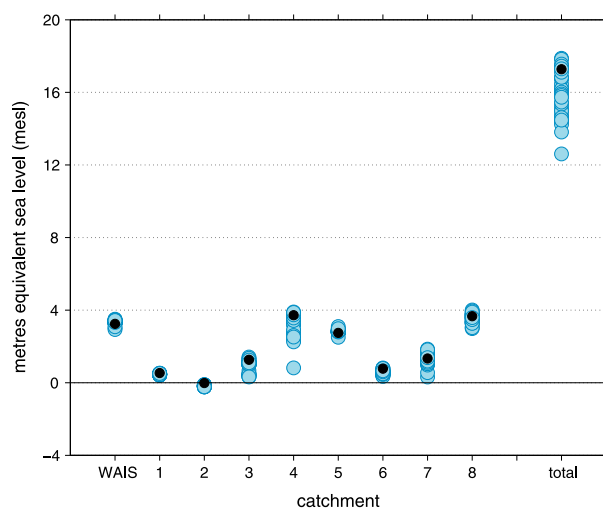


**Figure 4.** Sea level contribution from each catchment (from Figure 1) after 3 kyrs of warm climate simulation (difference between end of preindustrial simulation and end of warm climate simulation), black dots are for Bedmap2 best estimate simulation.

due to changing ice loads but ignores ice sheet gravitational effects on local sea level [Gomez *et al.*, 2010]. We perform ice sheet model simulations for all topographies with and without ice shelf hydrofracturing and ice cliff failure, using both the PD12 and PDA15 versions of the ice sheet model.

### 3. Results and Discussion

To avoid including ice volume changes created solely by the differences in topography, we calculate changes in ice sheet volume as the difference between the warm climate simulation after 3 kyrs and the end of the preindustrial control simulation for each topography. All sea level equivalent values are for ice over floatation and take into account the change in the state from ice to seawater. With the PD12 version of the model, the total loss of Antarctic ice varies from 1.6 to 3.5 mesl (metres equivalent sea level), largely from the loss of the WAIS. However, for the majority of PD12 simulations the total contribution from the EAIS is slightly negative ( $\sim -1$  mesl) due to increased precipitation. For the East Antarctic catchments the greatest loss comes from the Wilkes Subglacial Basin (within catchment 5 in Figure 1), which partially retreats for some simulations (up to 0.9 mesl, see Figure S2 in the supporting information).

For simulations using the PDA15 version of the ice sheet model, including both new physical mechanisms of retreat, there is significant retreat of the EAIS (see Figure 3), with a total Antarctic ice sheet loss of 12.6–17.9 mesl (compared with 17.3 mesl using the best estimate Bedmap2 topography, see Figure 4). For some of the regions with high bedrock elevation uncertainty (3, 7, and 8 in Figure 1) there is variable retreat, with the largest differences occurring in areas of high uncertainty, such as the Recovery and Support Force glaciers, and Princess Elizabeth Land. However, it is the Aurora Subglacial Basin (4) with relatively low bedrock elevation uncertainty which has the largest range across simulations (0.8–3.9 mesl, Figure 4). The majority of simulations have large-scale retreat into



the Aurora Subglacial Basin via the Denman Glacier and/or Sabrina Land. When using the best estimate Bedmap2 topography, retreat proceeds in both of these regions. In some instances retreat is into only one of these channels; however, this is sufficient to generate collapse of the Aurora Subglacial Basin.

Retreat into the Aurora Subglacial Basin is typically slower than for other regions, with 0.4–1.4 mesl of retreat after 1 kyr of warm climate forcing (with total Antarctic ice sheet loss after 1 kyr between 9.0 and 11.0 mesl). The slow initial retreat into the Aurora Subglacial Basin is due to the shallow marine bed of the surrounding coastal region, which generates relatively slow rates of retreat from the ice cliff failure mechanism. *Young et al.* [2011] identified deep paleo-fjords piercing the mountain ranges which border the Aurora Subglacial Basin. Although we do simulate retreat through these channels (seen in Figure 3 as gaps between the mountain ice caps that remain at the edge of the Aurora Subglacial Basin), retreat may be slower there due to the smoothing of these features by the 20 km model resolution. The fastest retreat is into the Recovery glacier system (up to 2.5 mesl after 1 kyr) and the Wilkes Subglacial Basin (up to 2.4 mesl after 1 kyr), which have deep troughs close to the coast.

Variations in bedrock elevation affect ice sheet stability due to a number of mechanisms within the ice sheet model. At the grounding line, ice flux is strongly controlled by ice thickness [Schoof, 2007]. In addition, the ice cliff failure mechanism is parameterized based on water depths. In these warm climate simulations with enhanced hydrofracturing and the ice cliff failure mechanism, retreat occurs in marine-based regions with sufficiently deep beds and continues until sufficiently shallow topography is reached. This is evident in the Wilkes Subglacial Basin, with the ice sheet stabilizing once the bed shallows. Small areas around the Aurora Subglacial Basin are close to a topography threshold where ice either retreats or remains stable. Therefore, despite the relatively low bedrock elevation uncertainty, the ice sheet model is very sensitive to changes in bed elevation in this region. If retreat proceeds beyond the shallow regions, then there is very large retreat into the deeper interior regions. It is possible that this threshold may be model dependent and sensitive to other parameters within the ice sheet model, but tests on a small subset of the topographies without the basal sliding parameter inversion produce similar results to those shown here, suggesting that it is the topography and not the basal sliding parameters that is driving the model sensitivity.

*Sun et al.* [2014] added random noise to the bedrock topography for three Antarctic regions (Pine Island bay, the Lambert-Amery system, and Totten-Denman system) to investigate how this affected ice sheet stability in the BISICLES ice sheet model, although at higher spatial resolution and over much shorter timescales than the simulations presented here. They found greater variability between simulations with lower frequency topographic noise. This contrasts with our simulations (see Figure S3), where ice sheet stability is not strongly affected by the frequency of the topographic noise.

Reconstructions of past Antarctic topography, for example, for the Eocene–Oligocene transition (EOT; ~34 Ma), suggest that Antarctic bedrock topography was very different in the past, with much shallower subglacial basins, presumably prior to the effects of large-scale glaciation [Wilson *et al.*, 2012]. Given the sensitivity of results in this study to bedrock elevation, it is likely that this would have implications for the past stability of the ice sheet on million year timescales. We have not addressed potential changes to the Antarctic bedrock since the Pliocene or for earlier periods of Antarctic instability (such as the EOT and mid-Miocene), or the impact of changes in local relative sea level on ice sheet stability. These will be the subject of future studies.

#### 4. Conclusions

Ice sheet models are sensitive to uncertainty in bedrock elevation. Present-day bedrock elevation uncertainty generates a range of responses in Antarctic ice sheet simulations for a warmer climate, analogous to the mid-Pliocene or to predicted future climate. The simulated retreat is equivalent to a sea level rise of 12.6–17.9 m, in an ice sheet model with mechanisms for ice shelf hydrofracturing and ice cliff failure after 3 kyrs of forcing. If the Greenland ice sheet also completely melted during the mid-Pliocene, this would create a total sea level rise of 20.0–25.3 m, which is comparable to some estimates of the Pliocene sea level highstand [e.g., Naish and Wilson, 2009; Miller *et al.*, 2012]. This model sensitivity is also relevant to long-term simulations of a future warm climate. Although some of the variation between our simulations is due to regions of high bedrock elevation uncertainty (such as the Recovery and Support Force glaciers), much is due to uncertainty in key areas of instability, such as the Denman Glacier and Sabrina Land. This suggests that future efforts to improve bedrock elevation estimates should be targeted in these regions in addition to reducing overall uncertainty.

## Acknowledgments

This study was supported by U.S. National Science Foundation award OCE-1202632 and AGS-1203910. The data used for this study are available upon request from the corresponding author (egw.gasson@gmail.com).

The Editor thanks two anonymous reviewers for their assistance in evaluating this paper.

## References

- Bassis, J. N., and C. C. Walker (2011), Upper and lower limits on the stability of calving glaciers from the yield strength envelope of ice, *Proc. R. Soc. A*, 468(2140), 913–931, doi:10.1098/rspa.2011.0422.
- Collins, M. R., et al. (2013), Chapter 12: Long-term climate change: Projections, commitments and irreversibility, in *Climate Change 2013: The Physical Science Basis. Contribution of Working Group I to the Fifth Assessment Report of the Intergovernmental Panel on Climate Change*, edited by T. F. Stocker et al., pp. 1029–1136, Cambridge Univ. Press, Cambridge, U. K. and New York.
- Cook, C. P., et al. (2013), Dynamic behaviour of the East Antarctic ice sheet during Pliocene warmth, *Nat. Geosci.*, 6(9), 765–769, doi:10.1038/ngeo1889.
- DeConto, R. M., D. Pollard, and D. Kowalewski (2012), Modeling Antarctic ice sheet and climate variations during Marine Isotope Stage 31, *Global Planet. Change*, 88–89, 45–52.
- Dowsett, H. J., M. M. Robinson, and K. M. Foley (2009), Pliocene three-dimensional global ocean temperature reconstruction, *Clim. Past*, 5, 769–783.
- Fretwell, P., et al. (2013), Bedmap2: Improved ice bed, surface and thickness datasets for Antarctica, *Cryosphere*, 7(1), 375–393, doi:10.5194/tc-7-375-2013.
- Gladstone, R. M., A. J. Payne, and S. L. Cornford (2012), Resolution requirements for grounding-line modelling: Sensitivity to basal drag and ice-shelf buttressing, *Ann. Glaciol.*, 53(60), 97–105, doi:10.3189/2012AoG60A148.
- Gomez, N., J. X. Mitrovica, P. Huybers, and P. U. Clark (2010), Sea level as a stabilizing factor for marine-ice-sheet grounding lines, *Nat. Geosci.*, 3, 850–853, doi:10.1038/NGEO1012.
- Holland, P. R., A. Jenkins, and D. M. Holland (2008), The response of ice shelf basal melting to variations in ocean temperature, *J. Clim.*, 21, 2558–2572.
- Mercer, J. H. (1978), West Antarctic Ice Sheet and CO<sub>2</sub> greenhouse effect: A threat of disaster, *Nature*, 271, 321–325.
- Miller, K. G., et al. (2012), High tide of the warm Pliocene: Implications of global sea level for Antarctic deglaciation, *Geology*, 40(5), 407–410, doi:10.1130/G32869.1.
- Naish, T. R., and G. S. Wilson (2009), Constraints on the amplitude of mid-Pliocene (3.6–2.4 Ma) eustatic sea level fluctuations from the New Zealand shallow-marine sediment record, *Philos. Trans. R. Soc. A*, 367(1886), 169–87, doi:10.1098/rsta.2008.0223.
- Naish, T., et al. (2009), Obliquity-paced Pliocene West Antarctic ice sheet oscillations, *Nature*, 458(7236), 322–328, doi:10.1038/nature07867.
- Nick, F. M., C. J. van der Veen, A. Vieli, and D. I. Benn (2010), A physically based calving model applied to marine outlet glaciers and implications for the glacier dynamics, *J. Glaciol.*, 56(199), 781–794, doi:10.3189/002214310794457344.
- Pal, J., et al. (2007), Regional climate modeling for the developing world: The ICTP RegCM3 and RegCNET, *Bull. Am. Meteorol. Soc.*, 88, 1395–1409.
- Pattyn, F., et al. (2013), Grounding-line migration in plan-view marine ice-sheet models: Results of the ice2sea MISIMP3d intercomparison, *J. Glaciol.*, 59(215), 410–422.
- Pollard, D., and R. M. DeConto (2012a), Description of a hybrid ice sheet-shelf model, and application to Antarctica, *Geosci. Model Dev.*, 5(5), 1273–1295, doi:10.5194/gmd-5-1273-2012.
- Pollard, D., and R. M. DeConto (2012b), A simple inverse method for the distribution of basal sliding coefficients under ice sheets, applied to Antarctica, *Cryosphere*, 6, 953–971, doi:10.5194/tc-6-953-2012.
- Pollard, D., R. M. DeConto, and R. B. Alley (2015), Potential Antarctic Ice Sheet retreat driven by hydrofracturing and ice cliff failure, *Earth Planet. Sci. Lett.*, 412, 112–121, doi:10.1016/j.epsl.2014.12.035.
- Pritchard, H. M. (2014), Bedgap: Where next for Antarctic subglacial mapping?, *Antarct. Sci.*, 26(6), 742–757, doi:10.1017/S095410201400025X.
- Raymo, M. E., J. X. Mitrovica, M. J. O'Leary, R. M. DeConto, and P. J. Hearty (2011), Departures from eustasy in Pliocene sea-level records, *Nat. Geosci.*, 4(5), 328–332, doi:10.1038/ngeo1118.
- Schoof, C. (2007), Ice sheet grounding line dynamics: Steady states, stability, and hysteresis, *J. Geophys. Res.*, 112, F03S28, doi:10.1029/2006JF000664.
- Seki, O., G. L. Foster, D. N. Schmidt, A. Mackensen, K. Kawamura, and R. D. Pancost (2010), Alkenone and boron-based Pliocene pCO<sub>2</sub> records, *Earth Planet. Sci. Lett.*, 292(1–2), 201–211, doi:10.1016/j.epsl.2010.01.037.
- Sun, S., S. L. Cornford, Y. Liu, and J. C. Moore (2014), Dynamic response of Antarctic ice shelves to bedrock uncertainty, *Cryosphere Discuss.*, 8(1), 479–508, doi:10.5194/tcd-8-479-2014.
- Thompson, S., and D. Pollard (1997), Greenland and Antarctic mass balances for present and doubled atmospheric CO<sub>2</sub> from the GENESIS version-2 global climate model, *J. Clim.*, 10, 871–900.
- Weertman, J. (1974), Stability of the junction between an ice sheet and an ice shelf, *J. Glaciol.*, 13(67), 3–11.
- Wilson, D. S., S. S. R. Jamieson, P. J. Barrett, G. Leitchenkov, K. Gohl, and R. D. Larter (2012), Antarctic topography at the Eocene-Oligocene boundary, *Palaeogeogr. Palaeoclimatol. Palaeoecol.*, 335–336, 24–34, doi:10.1016/j.palaeo.2011.05.028.
- Young, D. A., et al. (2011), A dynamic early East Antarctic Ice Sheet suggested by ice-covered fjord landscapes, *Nature*, 474(7349), 72–75.